J|A|C|S
ARTICLES
Published on Web 06/15/2006

Effect of Surface Composition on Electronic Structure, Stability, and Electrocatalytic Properties of Pt-Transition Metal Alloys: Pt-Skin versus Pt-Skeleton Surfaces

Vojislav R. Stamenkovic,*,† Bongjin Simon Mun,‡ Karl J. J. Mayrhofer,‡ Philip N. Ross,‡ and Nenad M. Markovic†

Contribution from the Materials Science Divisoin, Argonne National Laboratory, Argonne, Illinois 60439 and Materials Sciences Division, Lawrence Berkeley National Laboratory, Berkeley, California 94720

Received January 10, 2006; E-mail: vrstamenkovic@anl.gov

Abstract: The surface properties of PtM (M = Co, Ni, Fe) polycrystalline alloys are studied by utilizing Auger electron spectroscopy, low energy ion scattering spectroscopy, and ultraviolet photoemission spectroscopy. For each alloy initial surface characterization was done in an ultrahigh vacuum (UHV) system, and depending on preparation procedure it was possible to form surfaces with two different compositions. Due to surface segregation thermodynamics, annealed alloy surfaces form the outermost Pt-skin surface layer, which consists only platinum atoms, while the sputtered surfaces have the bulk ratio of alloying components. The measured valence band density of state spectra clearly shows the differences in electronic structures between Pt-skin and sputtered surfaces. Well-defined surfaces were hereafter transferred out from UHV and exposed to the acidic (electro)chemical environment. The electrochemical and post-electrochemical UHV surface characterizations revealed that Pt-skin surfaces are stable during and after immersion to an electrolyte. In contrast all sputtered surfaces formed Pt-skeleton outermost layers due to dissolution of transition metal atoms. Therefore, these three different near-surface compositions (Pt-skin, Pt-skeleton, and pure polycrystalline Pt) all having pure-Pt outermost layers are found to have different electronic structures, which originates from different arrangements of subsurface atoms of the alloying component. Modification in Pt electronic properties alters adsorption/catalytic properties of the corresponding bimetallic alloy. The most active systems for the electrochemical oxygen reduction reaction are established to be the Pt-skin near-surface composition, which also have the most shifted metallic d-band center position versus Fermi level.

1. Introduction

The need to understand the physicochemical properties governing the catalytic behavior of bimetallic alloy surfaces continues to provide a strong impetus toward fundamental studies of the surface processes at the electrified metal−solution interfaces.[1−5] The surface electrochemistry of Pt alloyed by the 3d-transition metals (Pt−M alloys, M = Co, Ni, Fe, etc.) is of particular interest, since these alloys are found to be 2−4 times more active than Pt-poly for the electrochemical oxygen reduction reaction (ORR),[6−12] which is the cathodic half-cell reaction in low temperature polymer electrolyte membrane (PEM) fuel cells. The possible explanation for the enhanced ORR activity on the bulk and high surface area Pt−M alloys was enumerated as being due to one or more of the following effects: (i) leaching out of 3d elements, resulting in a rougher Pt surface and thus a larger number of active sites (increase of the active surface area);[13,14] (ii) modification of the electronic structure of Pt (affecting the Pt−OH bond energetic);[11] (iii) change in the geometric structure of Pt (Pt−Pt bond distance and coordination number);[9] (iii) particle size effect and/or impediment of Pt crystal growth (coalescence of Pt nanoparticles);[15−17] (iv) wettability of the catalysts;[18] and/or (v) redox

† Argonne National Laboratory.
‡ Lawrence Berkeley National Laboratory.

(1) Ross, P. N., Jr. The Science of Electrocatalysis on Bimetallic Surfaces. In *Electrocatalysis*; Lipkowski, J., Ross, P. N., Jr., Eds.; Wiley-VCH: New York, 1998; pp 43−74.
(2) Markovic, N. M.; Ross, P. N. *Surf. Sci. Rep.* **2002**, *45*, 117−230.
(3) Norskov, J. K.; Rossmeisl, J.; Logadottir, A.; Lindqvist, L.; Kitchin, J. R.; Bligaard, T.; Jonsson, H. *J. Phys. Chem. B* **2004**, *108*, 17886−17892.
(4) Wang, J. X.; Brankovic, S. R.; Zhu, Y.; Hanson, J. C.; Adzic, R. R. *J. Electrochem. Soc.* **2003**, *150*, A1108−A1117.
(5) Roques, J.; Anderson, A. B. *Surf. Sci.* **2005**, *581*, 105−117.
(6) Luczak, F. J.; Landsman, D. A. U.S. Patent 4,447,506, 1984.
(7) Paffet, M. T.; Beery, G. J.; Gottesfeld, S. *J. Electrochem. Soc.* **1987**, *143*, 58.
(8) Mukerjee, S.; Srinivasan, S. *J. Electroanal. Chem.* **1993**, *357*, 201.
(9) Stamenkovic, V.; Schmidt, T. J.; Markovic, N. M.; Ross, P. N., Jr. *J. Phys. Chem. B* **2002**, *106*, 11970−11979.
(10) Paulus, U. A.; Scherer, G. G.; Wokaun, A.; Schmidt, T. J.; Stamenkovic, V.; Radmilovic, V.; Markovic, N. M.; Ross, P. N. *J. Phys. Chem. B* **2001**, *106*, 4181−4191.
(11) Stamenkovic, V.; Schmidt, T. J.; Ross, P. N.; Markovic, N. M. *J. Electroanal. Chem.* **2003**, *554*, 191−199.
(12) Gasteiger, H. A.; Kocha, S. S.; Sompali, B.; Wagner, F. T. *Appl. Catal., B* **2005**, *56*, 9−35.
(13) Paffet, M. T.; Beery, J. G.; Gottesfeld, S. *J. Electrochem. Soc.* **1988**, *135*, 1431.
(14) Watanabe, M.; Tsurumi, K.; Mizukami, T.; Nakamura, T.; Stonehart, P. *J. Electrochem. Soc.* **1994**, *141*, 2659−2668.
(15) Beard, B.; Ross, P. N., Jr. *J. Electrochem. Soc.* **1990**, *137*, 3368.
(16) Kinoshita, K. *Electrochemical Oxygen Technology*; John Wiley & Sons: New Vork, 1992.

type processes involving the first row transition alloying elements.[9] However, since the alloyed high surface Pt catalyst nanoparticles may have neither the same particle size nor shape as the Pt catalysts to which they were compared, a simple comparison of activity normalized by either mass or surface area is insufficient to identifying a true alloying effect. A more detailed discussion of this point, specifically in the case of Pt−Co and Pt−Ni catalysts, can be found in refs 10, 14, and 19. These complexities of supported nanocatalysts reinforce the need for using well-characterized materials as a benchmark[9,11] to identify the fundamental surface properties of Pt−M alloys at electrified interfaces.

In previous work in this laboratory, we investigated both well-defined bulk-electrode surfaces and supported nanocatalysts. As pointed out in refs 9−11 and 20, these systems show clear similarities but by no means identical behavior. It was clear from these studies that even with well-defined bulk electrode surfaces some important fundamental issues still need to be addressed: (i) the stability of 3d elements in the electrochemical environment; (ii) the effect of bulk concentration of 3d elements on the catalytic activity; and (iii) characterization of *surface* electronic properties of Pt−M catalysts and direct correlation to catalytic activity. The present study will view results on these important issues and demonstrate that (i) in contrast to sputtered surfaces the Pt-skin near-surface composition is stable in the potential region of interest for fuel cells; (ii) catalytic properties are strongly dependent on the M concentration in the subsurface atomic layers; and (iii) by systematic introduction of M into the bulk phase it is quite feasible to tune electronic surface properties and thus the catalytic behavior of these materials. Due to necessity to elucidate[12,21] fundamental surface behavior of Pt−M alloys, this study will explain the origin and enhanced catalytic behavior of Pt-skin and Pt-skeleton surface formations.

2. Experimental Section

2.1. Sample Preparation. Polycrystalline platinum−transition metal bulk alloys, with 25 atomic % of Co, Fe, and Ni (hereafter denoted as Pt_3M) and 50 atomic % of Co (hereafter denoted as PtCo), were prepared in an arc-melting furnace under an argon atmosphere. The crystal phase and chemical bulk composition of alloys were verified via X-ray diffraction and X-ray fluorescence spectroscopy, respectively. Before introduction into UHV, cylindrical samples with a diameter of 6 cm and a height of 4 cm were made by centerless grinding, polished to a mirror finish, and ultrasonically cleaned in detergent and in pyrodistilled water.

2.2. Surface Treatment and Characterization. We used two different UHV chambers for surface alloy characterizations. The first UHV system is operated under base pressure in the 1×10^{-10} Torr range, and it is equipped with an angular-resolving double pass cylindrical mirror analyzer (PHI-DPCMA Φ15-255GAR) with an electron source at its center. A UHV cleaning procedure was done by repeating sputtering−annealing cycles with Ar^+ and oxygen until Auger electron spectroscopy (AES) indicated that, for given experimental conditions, an ideally clean (carbon and oxygen free) surface was produced. AES spectra were recorded in a derivative mode using the 3 keV electron beam energy, 3 eV_{p-p} modulation, and -5 μA beam current in the range from 140 to 900 eV. To produce a different surface composition, clean samples were either annealed at 1000 K or mildly sputtered with a 0.5 keV beam of Ar^+ ions. The surface compositions of alloy samples were determined by low energy ion scattering spectroscopy (LEIS). LEIS spectra were taken with a Ne^+ beam energy of 1 keV with sample currents from 5 to 30 nA at a residual Ne pressure of 2.5×10^{-8} Torr. The scattering angle was 127°, and the incidence angle was 45°. A Φ04-303A differentially pumped ion gun was used to raster the Ne^+ ion beam over an approximately 3 mm × 3 mm surface area. The time of recording was 60 s/spectrum. The clean Pt reference sample was prepared in the same manner, i.e., conventional metallurgy preparation and pretreatment in UHV in exactly the same way, mild sputter cleaning and/or annealing.

2.3. Electronic Structure. The ultraviolet photoelectron spectroscopy (UPS) measurements were carried out in the second UHV chamber at the beamline 9.3.2 of Advance Light Source, Lawrence Berkeley National Laboratory. All UPS data were taken at a base pressure under 5×10^{-10} Torr using a hemispherical electron analyzer (Scienta SES-100). Upon the sample transfer to the UHV chamber, the cycle of ion sputtering and annealing was repeated until the signals of carbon and oxygen contaminants are not present in the XPS spectrum. UPS spectra are taken of each sputtered and annealed surface. The incident photon energy was 90 eV, and the energy resolution of the spectrum was 0.05 eV or less. All measurements were done at the normal emission direction from the sample surface. The integration background, i.e., Shirley background, was applied to the measured spectrum, and the center of the d-band was calculated from the background-subtracted spectrum.[22] For the accurate comparison of all spectra, the upper level of integration of background subtraction was fixed at the 10.0 eV binding energy position throughout all valence band spectra.

2.4. Electrochemical Treatment. All the electrochemical surface treatments in the present study were conducted on either mildly sputtered or annealed surfaces, which were transferred from UHV into a rotating ring-disk assembly (RRDE) and immersed in 0.1 M $HClO_4$ (Baker, Ultrex) under a potential control of ca. 0.05 V. Electrolyte was prepared with triple pyrodistilled water and thermostated at 293 and 333 K, by circulating water through a constant-temperature bath connected with a water jacket of a standard three-compartment electrochemical cell. The reference electrode was a saturated calomel electrode (SCE) separated by a bridge from the reference compartment. All potentials are referenced to the reversible hydrogen electrode potential (RHE) at the same temperature. Argon, oxygen, and hydrogen gases (Air Products, 5N8 purity) were bubbled through a glass frit into the electrolyte. The geometrical surface area of the disk electrode (well-characterized surface in UHV) was 0.283 cm^2, and all potentiodynamic surface exposures were done with a sweep rate of 50 mV/s. The active surface area in each case was established from a cyclic voltammogram recorded in an argon-purged electrolyte by integrating the charge in the hydrogen adsorption/desorption region, i.e., from 0.0 to 0.4 V. The durability of each surface was checked with prolonged (30 min) potential cycling between 0 and 1.4 V in argon-saturated electrolyte, followed by subsequent recording of corresponding voltammograms before, during, and after oxygen reduction reaction (ORR) experiments. Catalytic activities for ORR were established at 333 K in the potential range from 0 to 1.25 V. Experiments were performed in the rational time frame for RRDE measurements, lasting up to 4 h under the strictly controlled conditions.

3. Results and Discussion

3.1. UHV Characterization of PtM Alloys. 3.1.1. Surface Composition of Pt_xM_y Alloys. Although surface analysis of

(17) Markovic, N. M.; Radmilovic, V.; Ross, P. N. Physical and Electrocehmical Characterization of Bimetallic Nanoparticle Electrocatalysts. In *Catalysis and Electrocatalysis at Nanoparticle Surfaces*; Wieckowski, A., Savinova, E., Vayenas, C., Eds.; Marcel Dekker: New York, Basel, 2003; pp 311−342.
(18) Imahashi, J.; Horiba, T.; Muranaka, Y. U.S. Patent 5,350,643, 1994.
(19) Toda, T.; Igarashi, H.; Uchida, H.; Watanabe, M. *J. Electrochem. Soc.* **1999**, *141*, 968.
(20) Paulus, U. A.; Wokaun, A.; Scherer, G. G.; Schmidt, T. J.; Stamenkovic, V.; Markovic, N. M.; Ross, P. N. *Electrochim. Acta* **2002**, *47*, 3787−3798.
(21) Teliska, M.; Murthi, V. S.; Mukerjee, S.; Ramaker, D. E. *J. Electrochem. Soc.* **2005**, *152*, A2159−A2169.
(22) Mun, B. S.; Choongman, L.; Stamenkovic, V.; Markovic, N. M.; Ross, P. N. *Journal of Chemical Physics* **2005**, *122*, 184712−184714.

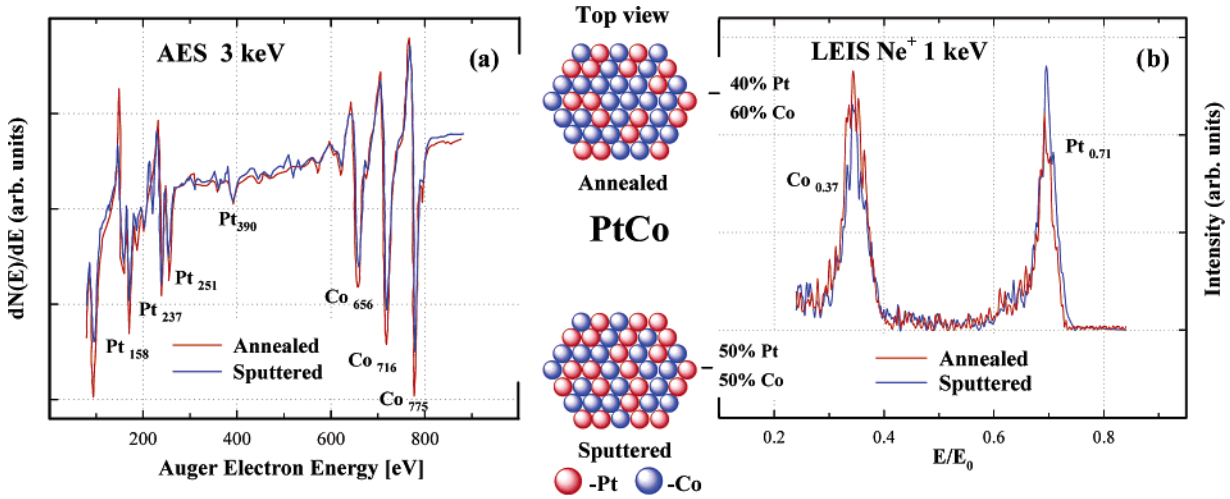

Figure 1. PtCo surface: (a) Auger electron spectra and (b) low energy ion scattering spectra. Mildly sputtered surface (blue curve) and annealed surface (red curve).

the Pt_3Co alloy has been described at some length previously,[9] selected AES/LIES results for Pt_3Co will be combined and compared with new AES/LIES analyses for the PtCo (1:1) alloy. Figure 1 shows typical AES and LEIS spectra of Pt_3Co obtained after either mild sputtering (blue curves) or annealing of specimen (red curves). In agreement with previous results for Pt_3Co,[9] the AES reveals that after sputtering/annealing cycles surfaces are free of impurities such as C and O and that the Co_{775}/Pt_{237} AES peak ratio decreases from 1.4 on the sputtered surface to 1 on the annealed surface. Although quantitative surface analysis of the Pt−M alloys with AES is quite complicated, requiring modeling of emission from several subsurface layers with dynamical scattering of the outgoing Auger electron, the fact that the Co_{775}/Pt_{237} AES peak ratio is different on sputtered and annealed surfaces may indicate that the concentration profile of Pt and Co atoms in the surface region may depend on the respective UHV pretreatment of the alloy. A true surface composition of the outermost atomic layer of the Pt_3Co alloy is obtained by utilization of LEIS, in which the scattering peaks of the Pt and Co atoms are calculated from the classical equation for elastic collisions.[23] By using the elemental sensitivity factors of polycrystalline materials,[24] we have been able to detect two different surface compositions depending on pretreatment; i.e., after mild sputtering the surface composition of the outermost atomic layer corresponds to the bulk ratio of alloying components (75 at. % of Pt and 25 at. % of Co), and after annealing the topmost surface layer consists of only Pt atoms. In accordance with $Pt_{80}Co_{20}(001)$ [25] and $Pt_{80}Co_{20}(111)$ [26] single-crystal studies, we proposed that in a polycrystalline Pt_3Co alloy there is analogous Pt enrichment due to segregation counterbalanced by the depletion of Pt atoms in the first two to three atomic layers underneath, resulting in a concentration profile which oscillates around the bulk value.[26] A pure topmost atomic layer of Pt has been designated as the *Pt*-skin surface [9;11]. The very same results have been found for all three Pt_3M alloys studied here, i.e., formation of a Pt-skin near-surface composition upon annealing.

Figure 1 summarizes AES and LEIS spectra of PtCo (50% of Pt and 50% of Co) alloy obtained after either mild sputtering (blue curves) or annealing of the specimen (red curves). There are two significant conclusions provided by the AES/LEIS results, which can make clear similarities and differences between Pt_3Co and PtCo alloy surfaces. Similar to the Pt_3Co system, the AES peak ratios as well as LEIS spectra of PtCo are dependent on the surface pretreatment. In contrast to Pt_3Co, for PtCo the Co_{775}/Pt_{237} peak ratio increases from 1.8 on the sputtered surface to 2 on the annealed surface, suggesting that the near-surface concentration of Co may increase upon annealing. Confirmation for the weak Co surface enrichment in the topmost layer of PtCo is obtained from LEIS spectra by comparing the Pt and Co signals for sputtered and annealed surfaces. As depicted in Figure 1b, on the annealed surface, a small yet clearly discernible increase of Co intensity is accompanied with a decrease of Pt peak intensity; see ball models in Figure 1. This is an important finding related to Pt segregation thermodynamics, which clearly depends on the bulk ratio of alloying components.

3.1.2. Electronic Surface Properties of PtM Alloys. The electronic structure of Pt, Pt_3Co, and PtCo sputtered and annealed surfaces are investigated with high-resolution ultraviolet photoelectron spectroscopy. Nørskov and co-workers[27−29] have suggested that a single metric, which captures the relationship between the electronic properties of metallic surfaces and the heat of adsorption of small molecules such as H_2, O_2, and CO, is the d-band center. The calculated d-band center and the measured UPS spectra are given in the Table 1 and Figure 2, respectively; i.e., the *p*th center of d-band calculation is defined as $\mu_p = \int N(\epsilon)\epsilon^p \, d\epsilon$, where $N(\epsilon)$ is the DOS (density of state) and p is the order of moment.[22] For example, μ_1/μ_0 is the first moment of DOS or its center of gravity. As shown in Figure 2 all systems exhibit spectra with a relatively broad maximum. The calculated positions of the

(23) Smith, D. P. *J. Appl. Phys.* **1967**, *38*, 340−347.
(24) Taglauer, E. *Appl. Phys. A* **1985**, *38*, 161−170.
(25) Bardi, U.; Atrei, A.; Zanazzi, E.; Rovida, G.; Ross, P. N., Jr. *Vacuum* **1990**, *41*, 437−440.
(26) Gauthier, Y. *Surf. Rev. Lett.* **2001**, *3*, 1663−1689.
(27) Hammer, B.; Norskov, J. K. Theory of Adsorption and Surface Reactions. In *Chemisorption and Reactivity on Supported Clusters and Thin Films*; Lambert, R. M., Pacchioni, G., Eds. Kluwer Academic Publisher: 1997; pp 285−351.
(28) Greeley, J.; Norskov, J. K.; Mavrikakis, M. *Annual Review of Physical Chemistry* **2002**, *53*, 319−348.
(29) Kitchin, J. R.; Norskov, J. K.; Barteau, M. A.; Chen, J. G. *Journal of Chemical Physics* **2004**, *120*, 10240−10246.

Table 1. Values for d-band Center Position Calculated from Corresponding UPS Spectra

alloy	Pt-poly [eV]	PtCo [eV]	Pt_3Co [eV]	Pt_3Fe [eV]	Pt_3Ni [eV]
sputtered surface	2.53 ± 0.01	2.74 ± 0.01	2.74 ± 0.01	2.89 ± 0.01	2.69 ± 0.01
annealed surface	2.54 ± 0.01	2.72 ± 0.01	2.86 ± 0.01	3.05 ± 0.01	2.72 ± 0.01

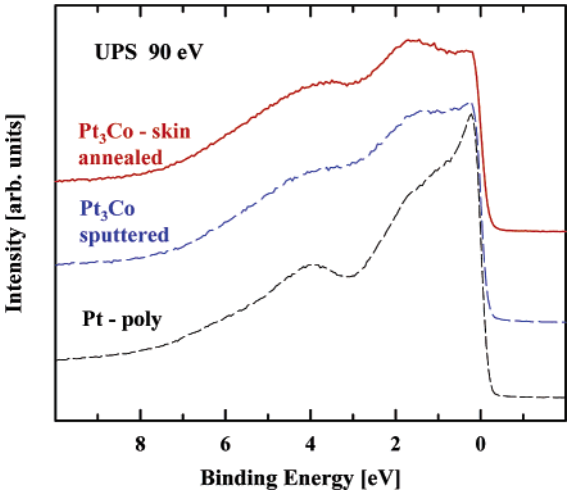

Figure 2. Background-subtracted valence band spectra of Pt_3Co surfaces: annealed Pt-skin surface (solid red curve), sputtered surface (dashed blue curve), and polycrystalline Pt surface (dashed black curve).

d-band center versus Fermi level, given in Table 1, are significantly different for all Pt−M surfaces than the value obtained for a polycrystalline Pt surface. The observed difference in d-band center position should be reflected in changes in the adsorption energies of reaction intermediates,[3,11,29,30] which can significantly alter catalytic properties of these surfaces.

3.2. Stability of Pt_xM_y Alloy Surfaces. The stability of PtM surface compositions after immersion in either a chemical or an electrochemical environment was investigated by ex situ surface analysis in UHV. Surface characterization of pretreated surfaces was done by utilizing AES and LEIS spectroscopy. Following (electro)chemical pretreatment, each well-characterized PtM alloy was rinsed with ultrapure triple distilled water, dried in an argon stream, and then transferred back to the UHV environment. Here it should be emphasized how demanding it is to maintain desired cleanliness of the surface during the transfer from UHV to (electro)chemical environment and then back to UHV.[32] Every consecutive step of surface treatment in and out of the UHV chamber should be done in an extremely careful manner to ensure the minimum exposure to potential contaminants. To reveal changes in the surface composition after (electro)chemical exposure, it is essential that no additional surface treatment is employed upon transfer back to the UHV, i.e., surface was not subjected to sputtering or annealing. Calibration, standardization, and optimization of our experimental procedure was initially done with a polycrystalline Pt sample, and the outcome after immersion into electro(chemical) environment was very usable AES spectra, having only a traceable signal for a carbon peak at 271 eV (check Figures 3a and 4a) with clearly pronounced Pt peaks. That was confirmation of the clean experimental conditions and properly optimized procedure. Since the Pt as a noble metal is considered to be stable and chemically resistant either in pure water or highly acidic/alkaline environments the crucial challenge in this study was to identify the surface chemistry/stability of transition metal atoms. In the topmost layer of all sputtered PtM alloys, non-platinum alloying components are present in the amount of 25 at. % or 50 at. % (PtCo system). To make this surface analysis more conclusive and unambiguous, the stability of Co surface atoms was tested first on a sputtered/annealed PtCo alloy with ca. 50 at. % of Co in the outermost atomic layer. The results from initial surface characterization of PtCo system are shown in Figure 1, and the set of data after exposure to the ultrapure water is given in Figure 3. From AES we found that while the Co_{775}/Pt_{237} AES peak-to peak ratio was very similar to that for a sputtered PtCo alloy depicted in Figure 1, after rinsing with water AES spectra indicated a significant presence of oxygen at 518 eV. Since the O_{518} peak is not observed after rinsing Pt with water, it is reasonable to conclude that the observed O_{518} peak rather comes from a Co-oxide formation than from a Pt-oxide or strongly adsorbed water molecules (to check the origin of the O_{518} peak, the sample was annealed at 420 K and no change in peak intensity was observed, indicating the presence of oxides adsorbed on Co sites rather than strongly adsorbed water molecules), as schematically shown in Figure 3 (black spheres). As a consequence of O and C presence on the surface in Figure 4a, there is obvious attenuation of both Pt and Co AES peaks relative to the C-free and O-free surface from Figure 1a. The confirmation that Co is stable and present on the surface is obtained from the LEIS spectra in Figure 3b, which clearly shows that Co surface atoms remained on the surface after rinsing with water indicating the same/similar ratio between Pt and Co peaks as in Figure 1b. Due to the noticeable presence of carbon impurities and oxygenated species (AES spectra in Figure 3a) LEIS spectra show increased intensities in the low E/E_0 region, which corresponds to the scattering of atoms having lower atomic numbers than Co.

The same PtCo surface (depicted in Figure 1) was immersed in the 0.1 M $HClO_4$ electrolyte under the potential control and then after five cycles between 0.05 and 1.0 V was transferred back into the UHV chamber for the AES/LEIS analysis. Interestingly, the AES and LEIS spectra of the PtCo surface emersed from an electrochemical cell (Figure 4) were identical with the results obtained after simply rinsing the surface with acidic electrolyte. In particular, AES of the surface rinsed with acid indicates a surface composition nearly free of O and C (based on AES sensitivity factors); the main features correspond only to Pt and Co. The fact that the AES signal for O in Figure 4a is significantly smaller after the emersion of PtCo from acid solution than from pure water indicates that in acid solution Co is dissolved from the surface. The same conclusion can be obtained from the relative ratio of Co_{775}/Pt_{237} peaks. In fact, a complete dissolution of surface Co atoms was revealed by the LEIS spectra shown in Figure 4b, which indicates that the outermost layer is indeed a *pure* Pt. It is clear that upon exposing

(30) Kitchin, J. R.; Khan, N. A.; Barteau, M. A.; Chen, J. G.; Yakshinskiy, B.; Madey, T. *Surf. Sci.* **2003**, *544*, 295−308.
(31) Evans, R. W.; Attard, G. A. *J. Electroanal. Chem.* **1993**, *345*, 337−350.
(32) Ross, P. N.; Wagner, F. T. The Application of Surface Physics Techniques to the Study of Elctrochemical Systems. In *Advances in Electrochemistry and Electrochemical Engineering*; Gerischer, H., Tobias, C. W., Eds.; John Wiley & Sons: 1984; pp 69−112.

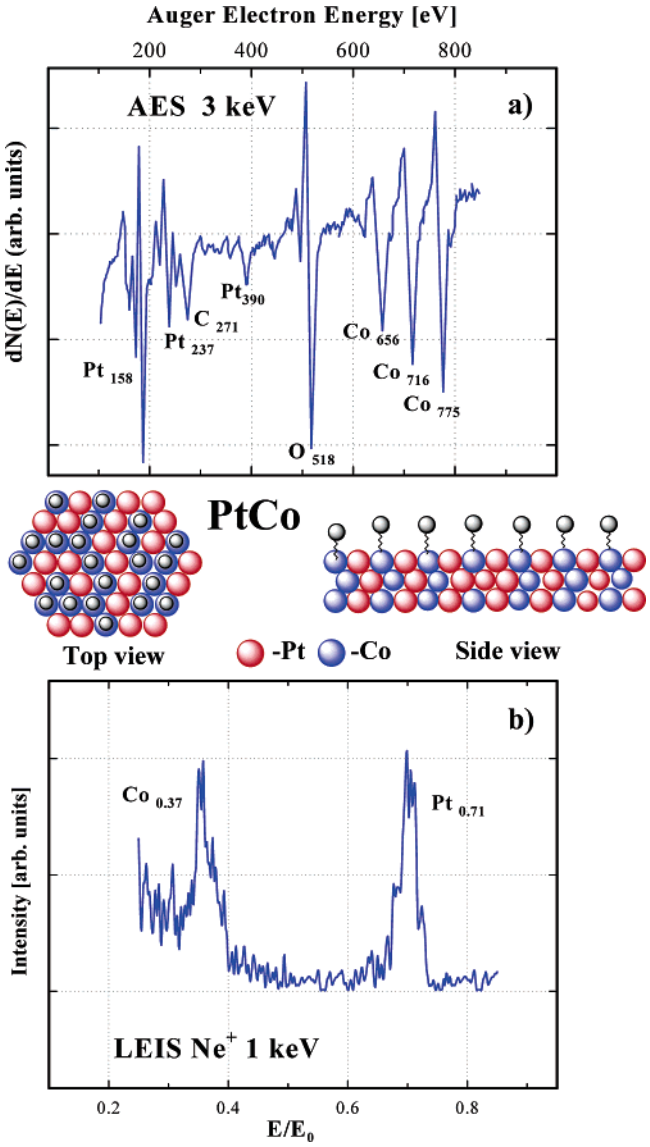

Figure 3. PtCo surface after exposure to H_2O: (a) Auger spectra reveal formation of stable oxides (black spheres), and (b) LEIS spectra confirm that Co content on the surface is the same upon transfer to the UHV.

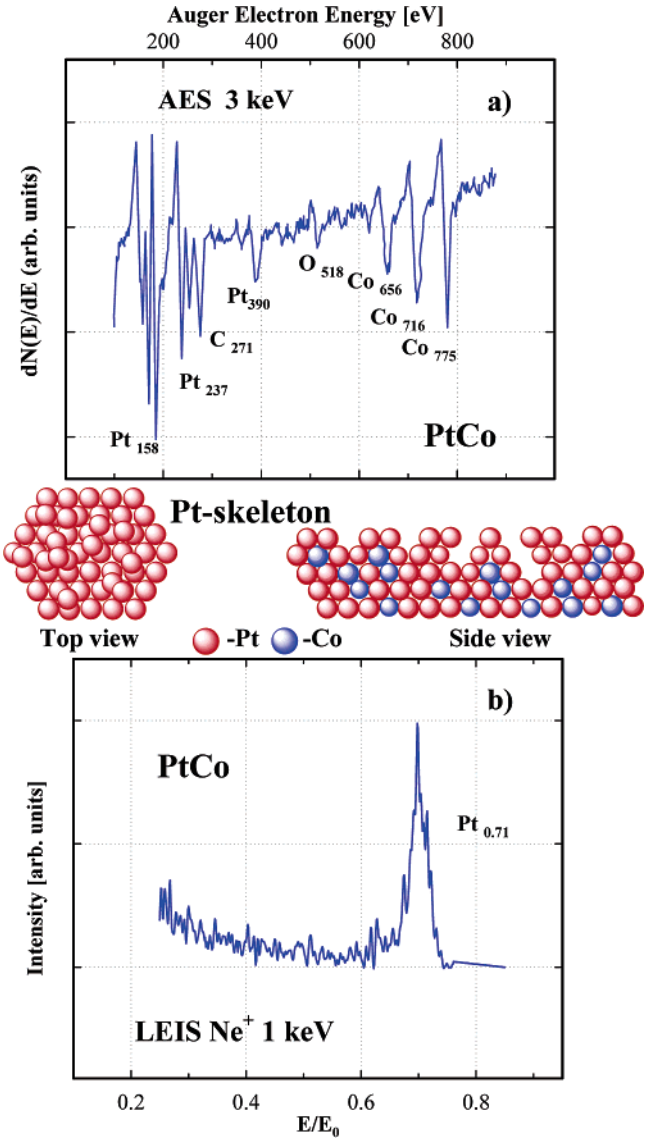

Figure 4. PtCo surface after exposure to 0.1 M $HClO_4$: (a) Auger electron spectra show decrease of Co peak intensity, and (b) low energy ion scattering spectra revealed that PtCo surface contains only Pt atoms in the topmost atomic layer after exposure to the electrolyte. Surface Co atoms are being dissolved forming the Pt-skeleton surface.

a PtCo surface with an initial surface composition of 50 at. % Pt and 50 at. % Co to an acidic solution, Co surface atoms are instantaneously dissolved from the near-surface layers. The remaining surface, which consists of only Pt atoms, after dissolution of alloying component we term a Pt-skeleton surface formation. That surface has been described previously in the literature by Watanabe et al.,[14] but it was designated as a skin of platinum with a thickness from 3 to 5 atomic layers determined by XPS measurements. It is important to mention that our definition of Pt-skin is different than the proposed notation in Watanabe's work, since we ascribed the term Pt-skin to the Pt topmost single atomic layer formed after annealing and Pt-skeleton to the surface remaining after dissolution of surface non-Pt atoms.

The conclusions drawn in this study from experiments with PtCo are, however, equally valid for the Pt_3Co, Pt_3Fe, and Pt_3Ni alloy sputtered surfaces. In each case, whenever transition metal atoms are exposed to the acidic environment, non-platinum atoms are dissolved forming a Pt-skeleton surface. There may be some differences between the alloys in the depth profile of transition metal atoms in the subsurface layers, but that determination was beyond the scope of this study. To this point it is the first known study, which relays on ex situ LEIS data as the most accurate surface sensitive tool for analysis of the topmost atomic layer and determination of the surface composition stability in the acidic environments. Comparison between data obtained on surfaces treated in water and acid (Figure 3b vs Figure 4b) unambiguously confirms a dramatic change in surface composition as well as the absence of a sputtering effect caused by the incident ion beam; i.e., intensity of the signal for Co at 0.37 does not change in the subsequent scans (Figure 3b), while for the same surface previously exposed to the acidic environment the Co peak does not exist (Figure 4b).

As mentioned above, the Pt-skin surfaces were formed over Pt_3M alloys after annealing at 1000 K due to complete segregation of Pt atoms.[9,11] The same set of ex situ analyses was performed on the Pt-skin surfaces formed over all three Pt_3M alloys. The fact that the AES/LEIS spectra after immersion to the (electro)chemical environment are identical (nearly free

of C and O) to those shown in Figure 1 (red curves) for the annealed Pt-skin surface supports our previous hypothesis[9,11] that the Pt-skin is stable in an (electro)chemical environment. This is an expected result, since the topmost layer already consists of only Pt atoms before exposure to the acidic environment. Our previously published results[9,11] showed stable behavior during the potential cycles in the range between 0.05 and 1.1 V. In the summary of this section, we conclude that in either the Pt-skin or Pt-skeleton surfaces, the pure Pt outermost layer protects the subsurface transition metal atoms from dissolution. That enables direct influence of an alloying component onto electronic properties of these unique Pt near-surface formations. These findings could be essential for understanding catalyst behavior during durability evaluations.[12]

3.3. Pt-Skin vs Pt-Skeleton vs Pt-Poly Surfaces. In our previous work[9,11] we established catalytic activity for an electrochemical oxygen reduction reaction on the same set of Pt alloy samples studied in this work. Due to the experimental limitations at that time, we could not relate the activity to the detailed surface/composition and proposed several possible explanations related to catalytic improvement. However, the present study brought essential clarification about the surface chemistry, stability of surface atoms, and the origin of catalytic improvement of alloyed surfaces. At this point we can rule out that roughening of the surfaces (increased surface area due to dissolution of alloying components) has a significant role in ORR activity enhancement. An experimental confirmation for this conclusion was obtained by comparison of the integrated hydrogen adsorption/desorption region derived from cycling voltammograms.[9] From these data, each of the Pt-skin (~180 μC/cm^2) and Pt-skeleton surfaces (~200 μC/cm^2) used in this study, has had lower surface coverage in hydrogenated species than the pure Pt-poly electrode (~220 μC/cm^2). That was a clear indication of changed adsorption properties for PtM systems and a negligible influence of the roughness factor (higher surface area). In addition our survey on electrochemical durability issues, which includes several hours of constant potential cycling and exposure to the positive potential limit up to 1.4 V (see Experimental Section), revealed no change in measured catalytic activities as well as no change in voltammetry features; i.e., the hydrogen adsorption/desorption region as well as oxide reduction peak remained the same before, during, and after electrochemical testing. That confirms stable surface behavior and consistent differences in activities in the electrochemical environment. Data reported here represent established values of specific activities for an oxygen reduction reaction obtained on stable and well-defined surfaces, as shown in Figure 5.

From these results Pt-skin surfaces were found to be the most active, followed by Pt-skeleton surfaces, and the least active surface was Pt-poly. Correlating measured values for ORR activity with UPS valence band measurements (Table 1), a direct link between surface electronic properties and intrinsic catalytic activity is clear. Therefore, the most active Pt-skin surfaces have the most pronounced shift of the d-band center induced by enrichment of the alloying component in the subsurface atomic layer relative to the bulk, so-called sandwichlike structure proposed for corresponding single-crystal alloys.[26,33,34] In

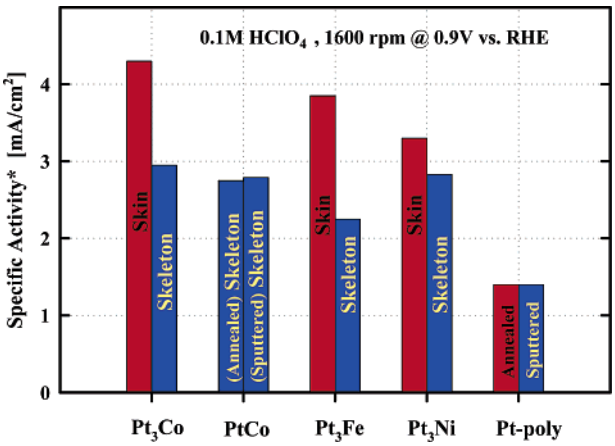

Figure 5. Specific activities (*expressed as kinetic current densities) for ORR measured on different Pt-skin and Pt-skeleton surfaces formed over corresponding Pt alloys. Measurements were done in 0.1 M $HClO_4$ with a rotation rate of 1600 rpm at 0.9 V vs RHE and 333 K.

contrast, Pt-skeleton ("leached-out") surface formations do not have an enriched subsurface layer in non-platinum atoms, and thus the level of electronic modification of the topmost Pt layer is not that pronounced as that for the Pt-skin, which drives a slower kinetic rate for ORR. The most pronounced skeleton effect is obtained for the PtCo (1:1) alloy, which forms a Pt-skeleton layer for both annealed and sputtered surfaces due to the absence of complete Pt segregation. Heavy dissolution of Co atoms takes place from several outermost atomic layers, which leads to the significant decrease of Co amount in the subsurface layers and rather weak influence of remaining Co onto remaining Pt-skeleton electronic properties. As a consequence the specific activity for the PtCo-skeleton is lower than that for the Pt_3Co-skeleton, which is also in accordance with d-band center position (see Table 1). The level of modification in electronic properties strongly depends on the presence of an alloying component in subsurface atomic layers and its nature; i.e., for observed Pt_3M alloys the highest catalytic activity is measured for Pt_3Co surfaces. Therefore, the lowest value of d-band center shift belongs to the Pt-poly surface, which is indeed the least active system for ORR. Although the exposed surface in all cases (Pt-skin, Pt-skeleton, and Pt-poly) consists of only Pt atoms, the arrangement of the surface and near surface atoms is different, which induces unique electronic modifications of a Pt outermost layer and, thus, different adsorption properties; i.e., catalytic properties are being changed. Adsorption properties are playing a key role in the kinetics of the oxygen reduction reaction. The surface coverage of adsorbates, which do not take place in the reaction mechanism, spectator/blocking species (oxides, anions etc) in the potential region relevant for ORR is different due to the electronically modified Pt topmost layer. The lowest value of the d-band center and thus the highest surface coverage by spectator species belong to the Pt-poly surface. Alloying of Pt brings a significant increase of d-band center position vs Fermi level (Table 1) and affects adsorption properties (weakens the adsorption strength between Pt and spectator species), which enables Pt-skin and Pt-skeleton surfaces to be less covered by spectator species and thus more active for ORR, i.e., more active sites for adsorption of molecular O_2. Therefore alloying Pt with different elements, in fact, leaves the possibility of tuning catalytic/electronic properties in the desired direction. The ORR enhancement factor of

(33) Gauthier, Y.; Baudoing, R.; Rundgren, J. *Phys. Rev. B* **1985**, *31*, 6216−6218.
(34) Gauthier, Y.; Baudoing-Savois, R.; Bugnard, J. M.; Bardi, U.; Atrei, A. *Surf. Sci.* **1992**, *276*, 1−11.

~2 established in this study (see Figure 5) on PtCo-skeleton surfaces vs Pt-poly very well agrees with the enhancement factor reported in ref 12, derived from testing of nanocatalysts under the fuel cell operating conditions. Based on that it is likely to conclude that a skeleton type of surface exists on nanoscale catalysts. These findings serve as a direct link between bulk and nanoparticle surfaces and can guide the design of advanced catalysts; i.e., the level of enhancement is in direct correlation with the type of the surface and should be used as a key parameter in tuning the surface−electronic−catalytic properties. A quantitative DFT analysis of the reaction mechanism and correlation between adsorption properties and the electronic structure of these surfaces are going to be the focus of our future report.

4. Conclusions

A detailed surface characterization study has been done on polycrystalline Pt bimetallic alloys, where alloying components were transition metals Co, Ni, and Fe. The bulk ratio between alloying elements were either 75 at. % Pt to 25 at. % M or 50 at. % Pt to 50 at. % M for PtCo system. In an ultrahigh vacuum environment for each Pt_3M alloy, depending on the preparation procedure, it was possible to form surfaces with two different compositions: (a) a Pt-skin surface after annealing at 1000 K due to complete segregation of Pt atoms, i.e., surface composition of 100 at. % Pt; and (b) after an ion sputtering procedure surface composition corresponds to the ratio of alloying components in the bulk 75 at. % Pt and 25 at. % M. Electronic properties, expressed as the shift of metallic d-band center vs Fermi level, are different for those two surfaces. For each Pt_3M alloy, the corresponding Pt-skin surface has a larger d-band center shift than the sputtered surface. The pure polycrystalline Pt surface has the lowest measured value for the d-band center position. Initial UHV characterization was followed by transfer of each well-defined surface to an (electro)chemical environment. After immersion to acidic electrolyte samples were rinsed with ultrapure water and transferred back to the UHV chamber for further surface analysis. Surface composition of the Pt-skin was found to be stable and consistent with values obtained during initial characterization. Opposite to that all sputtered surfaces after immersion to an acidic electrolyte exhibit significant change in the surface composition. All surface and near surface non-platinum atoms are dissolved instantaneously upon contact with an electrolyte leading to formation of the so-called Pt-skeleton surface with a surface composition of 100 at. % Pt. These surfaces with nominally the same surface composition (100 at. % Pt) are established to have different catalytic properties in the following order: Pt-skin > Pt-skeleton > pure Pt-polycrystalline. This trend in activity we ascribed to the modification of the surface electronic properties expressed as a position of the metallic d-band center vs Fermi level; i.e., adsorption properties of the surface are in direct correlation with the d-band center position.

Acknowledgment. This work was supported by the Director, Office of Science, Office of Basic Energy Sciences, Division of Materials Sciences, U.S. Department of Energy under Contract No. DE-AC03-76SF00098. We acknowledge the support of General Motors Corporation and helpful discussions with Hubert Gasteiger, Fred Wagner, and Shyam Kocha. Authors acknowledge Mark W. West for support in experimental design.

JA0600476